# scientific reports



### **OPEN**

# Effects of ultrasonic modification on physicochemical and structural properties of pomelo peel soluble dietary fiber extracted by alkali

Yang Ye¹, Fei Chen¹, Zhaoyi Lu¹, Jingyu Xiang¹, Guixiang Jia¹, Mingyi Xu², Yang Liu², Yang Wang¹⊠ & Xiaoling Wang²⊠

Pomelo peel, as a by-product of pomelo, is abundant with in soluble dietary fiber (SDF). The SDF obtained from pomelo peel using an alkaline solution was labeled ASDF, and the ASDF that was modified using ultrasound was labeled UASDF. An investigation was conducted into the physicochemical, structural, and functional properties of the samples were investigated. The investigative results show that ultrasound modification increases SDF content from 24.0 to 28.9%, with an improvement in the water-holding and swelling capacity of SDF. However, there is little effect on the oil-holding capacity. As revealed by the structural characterization both ASDF and UASDF exhibit the typical characteristics of cellulosic polysaccharides, but UASDF is 5.63% less crystalline than ASDF, resulting in a looser porous structure. In addition, UASDF possesses high glucose adsorption capacity (29.98 mg/g) and high cholesterol adsorption capacity in the small intestine (pH = 2, 20.86 mg/g; pH = 7, 25.11 mg/g). UASDF also exerts a more significant antioxidant effect, particularly ABTS free radical scavenging rate of 80.97% (5 mg/mL). The superior adsorption capacity and antioxidant ability of UASDF are attributed to its structure. These results demonstrate that pomelo peel is applicable as an inexpensive natural dietary fiber, and that UASDF possesses excellent functional characteristics.

**Keywords** Pomelo Peel, Soluble dietary fibers, Ultrasonic modification, Physicochemical properties, Structural characteristics

Pomelo, one of the most popular fruits in China, is consumed in large amounts annually. Pomelo peel accounts for 50% of the total of weight pomelo, but a great deal of pomelo peel was discarded as a by-product during pomelo processing, which leads to resource wastage and environmental pollution<sup>1</sup>. Containing various bioactive substances such as flavonoids, and essential oils, pomelo peel is rich in dietary fibers<sup>2</sup>. According to a study the dietary fiber content reaches as high as 63.47%, of which 14.82% is soluble dietary fiber and 50.99% is insoluble dietary fiber<sup>3</sup>. Therefore, pomelo by-products are considered a good source of dietary fiber.

Dietary fiber (DF), an indigestible carbohydrate derived from plant sources, as well as the seventh nutrient, plays an important physiological role in human body<sup>3,4</sup>. According to the solubility in water, dietary fiber can be classified as insoluble dietary fiber (IDF) and soluble dietary fiber (SDF)<sup>5</sup>. In comparison to IDF, SDF possesses superior beneficial properties for human health, such as water/oil holding capacity (WHC/OHC), water swelling capacity, hypoglycemic capacity, and lowering blood cholesterol content<sup>6–8</sup>. To make better use of SDF in the food industry, it is crucial to improve the yield of plant SDF and explore its properties.

The methods of SDF extraction methods include chemical, enzymatic, and fermentation methods. Some processing methods affect the composition and microstructure of the SDF, which in turn affects its functional properties. Among these methods, enzymatic extractions obtain more stable SDF but at high costly. Fermentation methods are economical but time-consuming. Alkali extraction is widely practiced in the dietary fiber industry, which allows for the removal of protein from residual and the generation of high purity dietary fiber<sup>9</sup>, despite at a low extraction rate. Ultrasonic waves are widely applied in the extraction process. As an effective method of extracting SDF, ultrasound-assisted extraction technique produces bubbles through cavitation, thus causing the fragmentation of the cellular structure, facilitating the contact with the solvent and improving the extraction

¹School of Biological Engineering, Sichuan University of Science and Engineering, Yibin 644005, China. ²Zigong First People's Hospital, Zigong 643000, China. ⊠email: dhwy518@163.com; 908189357@qq.com

rate<sup>10</sup>. Notably, it has been adopted for the extraction, and modification of SDF from most plant wastes, such as corn bran<sup>11</sup>, corn bract<sup>12</sup>, pineapple waste<sup>13</sup>, and Okara (soybean residue)<sup>14</sup>, etc. In the above process, the ultrasound-assisted technique not only increases the yield of SDF, but also beneficially alters the WHC, OHC, adsorptive properties (for glucose and cholesterol), and antioxidant characteristics of SDF. In addition, the SDF obtained by the modification method has been used to fortify functional foods (breads, cookies) and as a fat replacement. The in vitro digestive glucose release rate of bread was significantly reduced by the addition of modified grapefruit peel soluble dietary fiber<sup>15</sup>. Derived from the yellow dragon fruit rind species applied to alpaca-based sausage, SDF can be substituted with 78% fat content while its textural characteristics are maintained<sup>16</sup>. Therefore, the ultrasound-assisted alkali extraction technique not only compensates for the shortcomings of the single extraction method but also improves the yield of SDF through a synergistic effect.

The aim of this study was to use ultrasonic modification to prepare alkali-extracted soluble dietary fiber (SDF) from pomelo peel with increased yield and improved functional properties. This study compares the physicochemical, structural, and functional properties of the two SDFs, and investigates the relationship between these properties and their functions. This provides a novel idea for studying pomelo peel SDF and offers a theoretical reference for the comprehensive utilization of pomelo peel.

#### Results and discussion Extraction yield

As shown in Table 1, compared with alkali extraction (ASDF, 24.00%), ultrasound-assisted alkali extraction (UASDF, 28.90%) of SDF from pomelo peel is higher. According to the results, the ultrasonic-assisted extraction of alkali extraction is effective in improving the extraction rate of SDF.

#### Physicochemical properties

The capability of pomelo peel fibers to hold water and oil is crucial for food applications. The WHC, OHC, and SC of SDF were influenced by several factors, primarily including its structure, porosity, and particle size  $^{17}$ . Table 1 lists WHC, OHC, and SC of ASDF and UASDF. The WHC and SC of UASDF ( $62.67\pm0.67$  g/100 g,  $3.26\pm0.05$  mL/g) are higher compared to ASDF ( $57.33\pm0.54$  g/100 g,  $1.07\pm0.03$ mL/g). Due to the generation of porous structures in UASDF, there is an increase in WHC and SC, which improves the ability to capture water in the teak SDF fiber matrix. Additionally, the OHC of ASDF and UASDF is  $10.96\pm0.43$  and  $11.13\pm1.27$  g/100 g, respectively. The OHC of both SDFs varies slightly changed, indicating that ultrasonic treatment has no effect on the interaction between SDFs and lipids  $^{18}$ . It is implied that the dietary fiber high in WHC acts as a functional ingredient to change the viscosity and texture of certain prepared foods. High OHC is associated with the stability of high-fat foods and emulsions  $^{19}$ .

#### Structural properties

FTIR spectra of the obtained SDF

Infrared spectroscopy was performed to analyze the structure of soluble dietary fiber derived from pomelo peel. The functional groups and chemical structures of ASDF and UASDF samples were determined by FT-IR (Fig. 1). Both SDF and UASDF exhibit FT-IR spectra characteristic of polysaccharides, despite the slight deviations in the position and intensity of absorption peak. The strong and broad absorption peak at 3441 cm<sup>-1</sup> for is associated with the O-H stretching vibrations that result mainly from cellulose and hemicellulose. The peaks at 2931 cm<sup>-1</sup>, 1412 cm<sup>-1</sup>, and 1396 cm<sup>-1</sup> belong to the C-H stretching vibration, which is a typical structure of fibrous polysaccharides<sup>8,20</sup>. The peaks at 1627 cm<sup>-1</sup> and 1629 cm<sup>-1</sup> for ASDF and UASDF, respectively, are ascribed to the interaction of glucuronide with C=O bonds. The peaks at 1039 cm<sup>-1</sup> and 1018 cm<sup>-1</sup> are attributed to the stretching vibrational peaks of the C-O bond, due to the presence of C-O-H and C-O-C in the cellulose and hemicellulose, or the blending vibrations of the primary alcohols<sup>21</sup>. Characteristic of  $\beta$ -glycosidic bonds, the small, sharp bands at 871 cm<sup>-1</sup> and 830 cm<sup>-1</sup> are present in hemicellulos<sup>22</sup>. The presence of these bands and peaks confirms the typical polysaccharide functional groups of ASDF and UASDF extracted from pomelo peel. There is a larger O-H peak area in UASDF, suggesting the more intramolecular hydrogen bonding and the higher hydrophilicity as a result. This aligns with the WHC and SC results.

#### X-ray analysis

X-ray diffraction was performed to assess the changes in crystallinity and thus to determine the aggregation state of the SDF molecules<sup>23</sup>. Figure 2 shows the spectra for ASDF and UASDF revealing that the main peaks are observable around 22° and 30°, with some non-crystalline secondary peaks at other angles. According to this result, the two SDFs are cellulose type I structures, with the coexistence of crystalline and amorphous regions<sup>24</sup>.

Sample <sup>1</sup>	ASDF	UASDF
Extraction yield(%)	$24.00 \pm 0.14^{b}$	$28.90 \pm 0.38^a$
WHC (g/100 g)	57.33 ± 0.54 <sup>b</sup>	$62.67 \pm 0.67^{a}$
SC (mL/g)	1.07 ± 0.03 <sup>b</sup>	$3.26 \pm 0.05^{a}$
OHC (g/100 g)	10.96 ± 0.43 <sup>a</sup>	11.13 ± 1.27 <sup>a</sup>

**Table 1**. Yield and physicochemical properties of ASDF and UASDF. <sup>1</sup>ASDF, the soluble dietary fiber obtained by alkali extraction; UASDF, the soluble dietary fiber obtained by ultrasound-assisted alkali extraction. <sup>a,b</sup>Different letters in the same row indicate significant differences (P < 0.05).

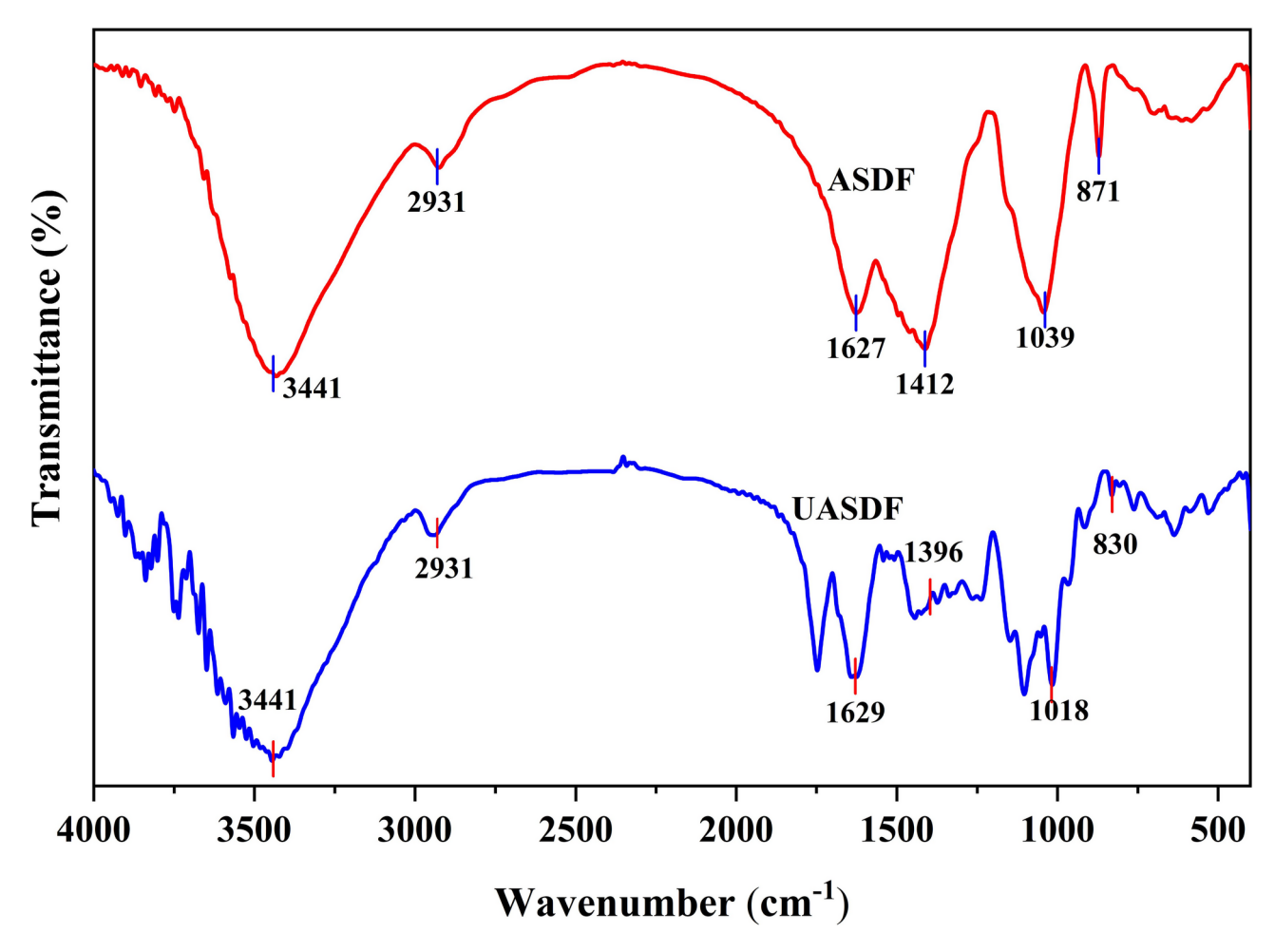


**Fig. 1**. FT-IR spectra of ASDF and UASDF. *ASDF* the soluble dietary fiber obtained by alkali extraction, *UASDF* the soluble dietary fiber obtained by ultrasound-assisted alkali extraction.

UASDF is similar to the crystalline form of ASDF, which indicates a failure of ultrasound to change the crystal type of ASDF. However, the crystallinity of UASDF (17.65%) is lower compared to ASDF (23.28%), which is possibly attributed to the partial intramolecular hydrogen bonds of ASDF being disrupted by ultrasound, which increases the amorphous region<sup>25</sup>. Ultrasonic treatment transforms the crystal structure from ordered to more disordered or even disordered, leading to the increased amorphous regions. These special structures could increase the relative surface area, which enhances glucose adsorption capacity (GAC) and cholesterol adsorption capacity (CAC). A similar result was obtained from Dhar and Deka<sup>13</sup> ultrasound-assisted alkali-treated Okala SDF.

#### SEM analysis

The surface microstructure plays an important role in the functional properties of SDFs, especially the adsorbing capacities of carbohydrates and cholesterol<sup>5</sup>. The SEM images mainly show the surface structure of ASDF and UASDF samples (Fig. 3). At 200x magnification, SDF samples exhibit a discontinuous and irregular overall structure, which is possibly due to alkali treatment removing binding proteins in large amounts<sup>26</sup>. At 3000x magnification, ASDF possesses a large blocky structure and a densely textured wrinkled surface, while the surface of UASDF is a small, loose, and porous structure. Compared with ASDF, UASDF has a larger specific surface area and porous structure, which may results in the absorption of ultrasonic energy by the cells. Consequently, cell rupture occurs and loose porous structures develop<sup>22,27</sup>. The ultrasonic modification treatment alters the structure of SDF, which results in the exposure of more polar and non-polar groups, promotes water absorption and swelling<sup>24</sup>, and improves the capability of SDF to absorb glucose, cholesterol and other harmful substances.

#### **Functional properties**

Glucose adsorption capacity (GAC) and cholesterol adsorption capacity (CAC) analysis

GAC is considered a significant functional property of SDF, which adsorbs glucose from intestinal fluids, thus reducing postprandial blood glucose levels<sup>28</sup>. As shown in Fig. 4A, UASDF had a higher GAC value (29.98 mg/g) than ASDF (24.17 mg/g). The porous structures of pomelo peel SDF obtained through ultrasonic extraction can adsorb more glucose and reduce blood sugar levels in the gut<sup>29</sup>. As for ASDF, the GAC values of ASDF are

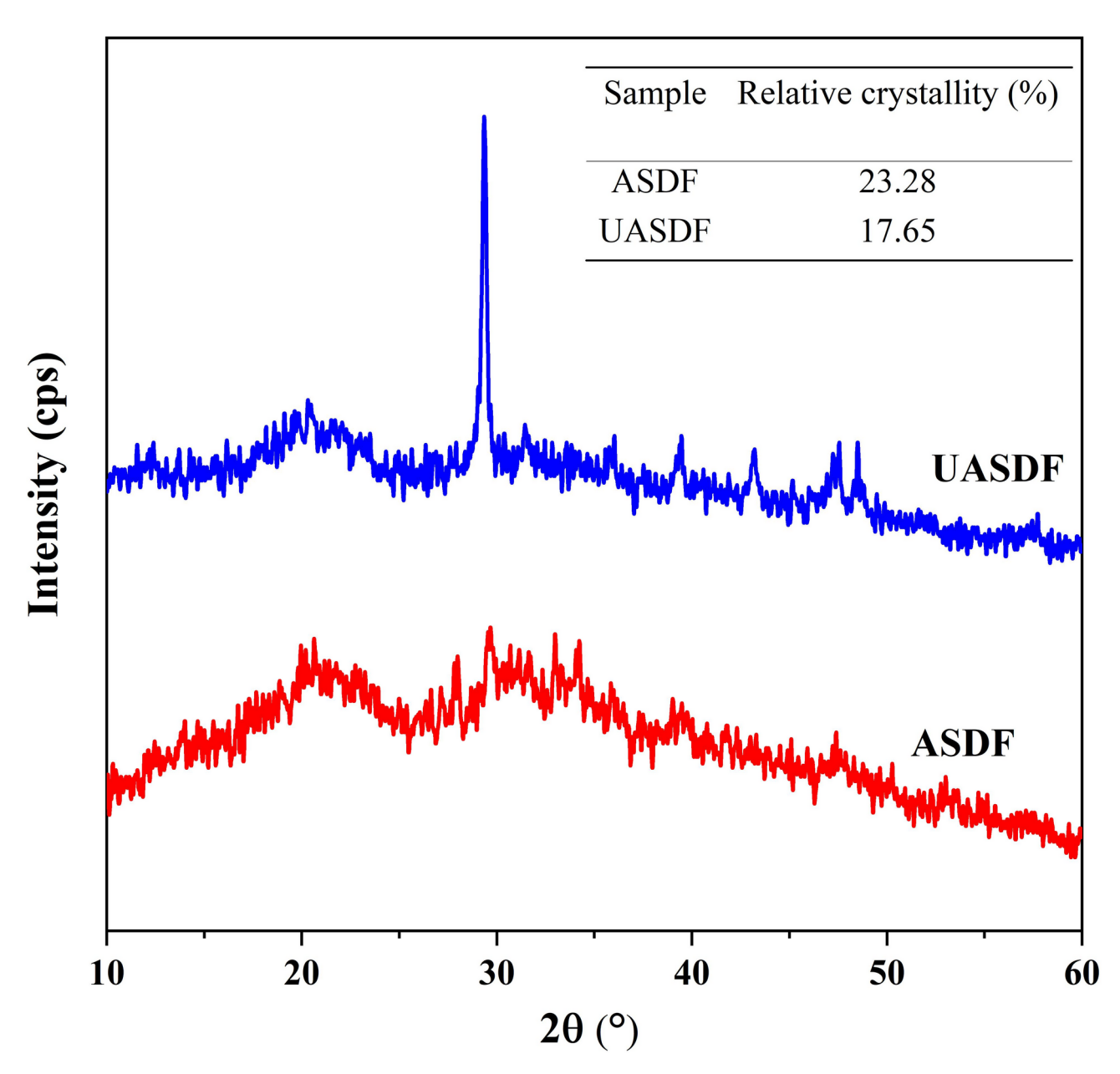


**Fig. 2.** The X-ray diffraction patterns of ASDF and USDF. *ASDF* the soluble dietary fiber obtained by alkali extraction. *UASDF* the soluble dietary fiber obtained by ultrasound-assisted alkali extraction.

consistent with the X-ray and SEM results. Besides, the high crystallinity and dense fibrous regions hinder the molecules of glucose from penetrating its interior, as a result of which it is more difficult to adsorb glucose<sup>30</sup>.

Figure 4B shows the binding capacity of SDF for cholesterol (at pH 2.0 and pH 7.0). From this figure, it can be seen the binding capacity of UASDF (pH=2.0, 20.86 mg/g; pH=7.0, 25.11 mg/g) for cholesterol is higher than that of ASDF (pH=2.0, 19.09 mg/g; pH=7.0, 18.66 mg/g), which may be attributable to the loose structure of dietary fibers and the increased surface area<sup>31</sup>. For UASDF, the binding ability for cholesterol is higher at pH 7.0 than at pH 2.0, with the opposite result was obtained for ASDF, despite no significant difference. The results demonstrate that UASDF creates greater health benefits in reducing cholesterol concentration in the small intestine, which is basically consistent with the previous findings of Peng et al., Luo et al., and those of Xu et al.<sup>32–34</sup>. In addition, this suggests that the fibers high in GAC and CAC can be applied as a functional component in lowering blood glucose and cholesterol in the body.

#### Scavenging capacity of ABTS, DPPH, and OH radicals

In this study, DPPH, ABTS, and ·OH free radical scavenging capacities were analyzed to evaluate the antioxidant capacity of SDF extracted by two methods at different concentrations. The scavenging capacity of DPPH free radicals is related to the hydrogen-donating capacity<sup>35</sup>. The scavenging rate of ABTS free radicals reflects the

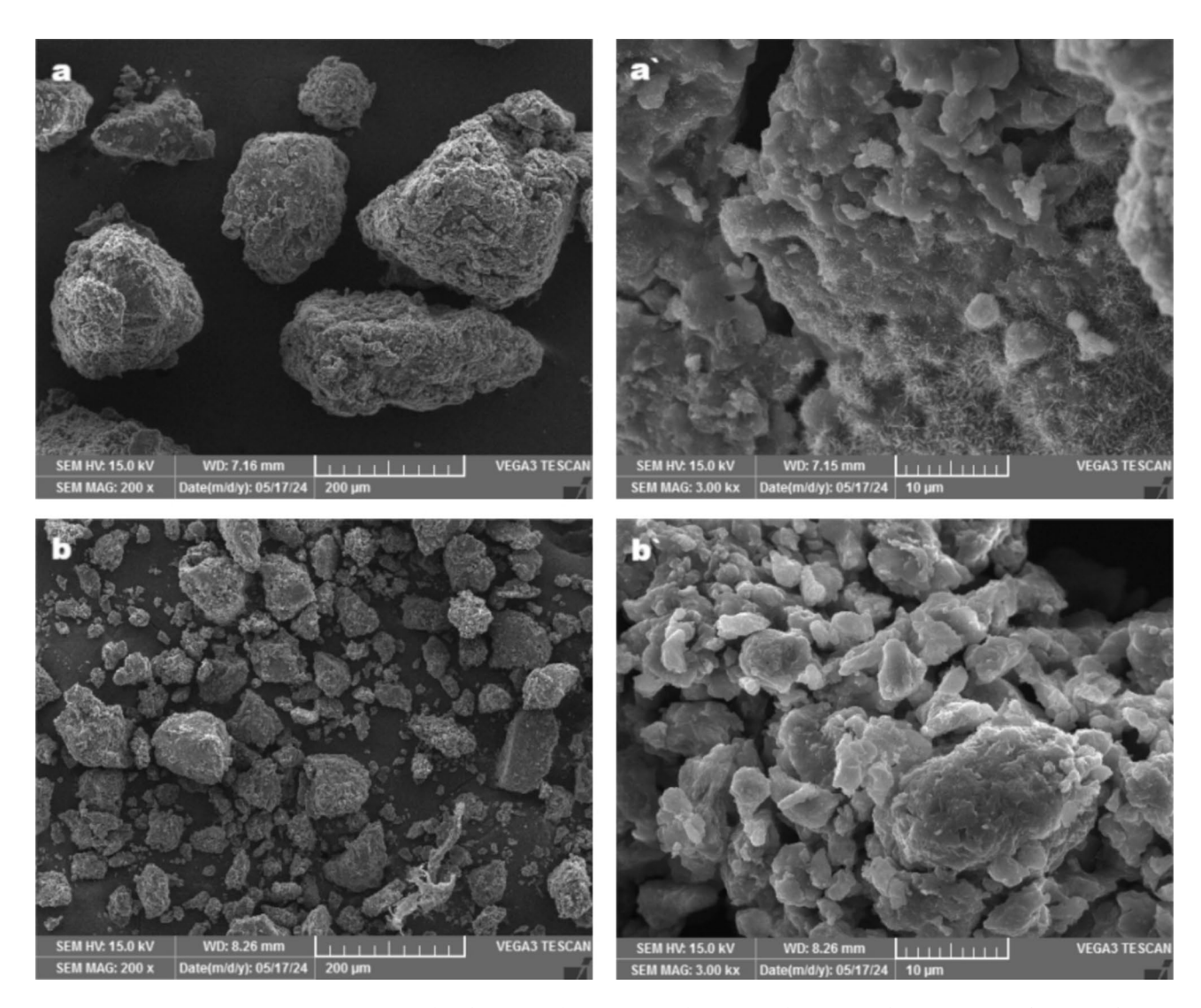


**Fig. 3.** SEM micrographs of ASDF and USDF. (a) and (a') were the images of ASDF at magnifications of 200x and 3000x. (b) and (b') were the images of UASDF at the magnifications of 200x and 3000x. *ASDF* the soluble dietary fiber obtained by alkali extraction, *UASDF* the soluble dietary fiber obtained by ultrasound-assisted alkali extraction.

electron and proton transfer capacity of the antioxidant<sup>26</sup>. Hydroxyl radical scavenging capacity is determined by hydrogen atom transfer<sup>36</sup>. They are useful to evaluate the free radical scavenging capacity of antioxidants.

The results shown Fig. 5A and 5B, and 5C are similar, with SDF scavenging three free radicals in a dose-dependent manner in a dose-dependent manner when there is an increase from 1 mg/mL to 5 mg/mL. As shown in Fig. 5A, it is notable that from 1 mg/mL to 4.53 mg/mL, the DPPH radical scavenging capacity of ASDF is higher than UASDF. At 5 mg/mL, the scavenging capacity of DPPH radicals of UASDF (80.97%) is higher than that of ASDF (75.06%). In spite of this, both are smaller compared to ascorbic acid (VC) (1 mg/mL, 91.58%). When SDF concentrations falls below 4.52 mg/mL, the hydrogen supply capacity in the UASDF is insufficient for the adequate reaction adequately with free radicals, as a result of which the antioxidant capacity declines<sup>37</sup>.

According to Fig. 5B, at 5 mg/mL, the scavenging capacity of ASDF and UASDF for ABTS radicals is 44.89% and 76.36%, respectively, both of which are lower than that of VC (99.18%, 1 mg/mL). The ABTS free radical scavenging rate of UASDF is nearly twice as high as that of ASDF. The scavenging of hydroxyl radicals by ASDF and UASDF is enhanced slowly with concentration, but both are smaller than VC (2 mg/mL, 88.05%). As shown in Fig. 5C, the hydroxyl radical scavenging rates of ASDF and UASDF are 44.45% and 51.12% at 5 mg/mL, respectively. The high ABTS and ·OH radical scavenging capacity of UASDF is attributable to the reduction in molecular weight and large surface area caused by ultrasonic treatment, which in turn improves the antioxidant properties and affects the glyoxylate content of the dietary fiber<sup>29</sup>. This result aligns with the FTIR result that indicates a strong absorption peak at a wavelength of 1629 cm<sup>-1</sup>. Moreover, the results are consistent with the findings of Wei et al.<sup>38</sup> that the antioxidant capacity of pomelo peel SDF is improved after the extraction by ultrasonic treatment. The fiber with high antioxidant activity as a functional ingredient maintains the stability of fatty foods, thus improving oxidative stability and extending the shelf life<sup>19</sup>.

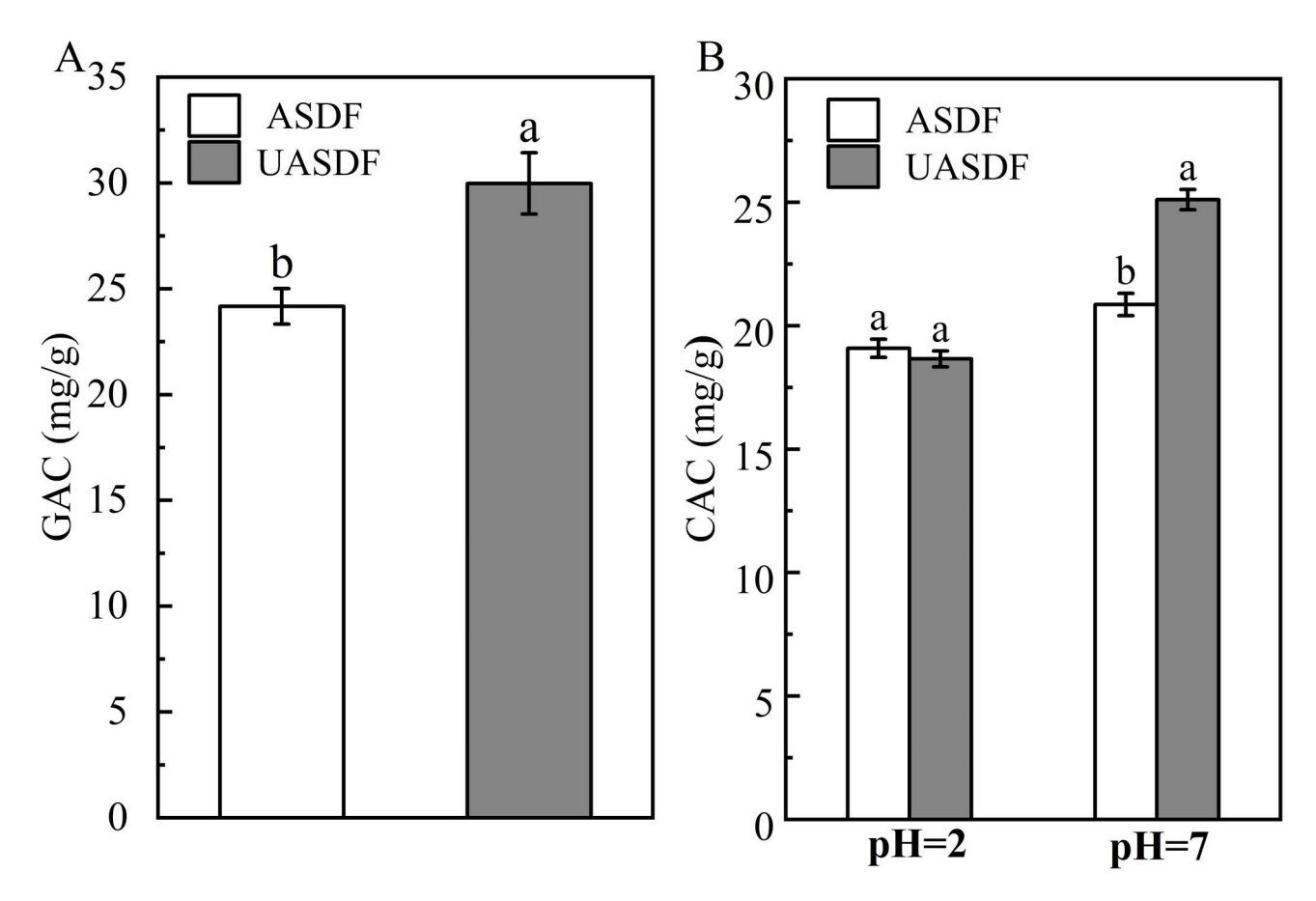


**Fig. 4.** The values of GAC (**A**) and CAC (**B**) of ASDF and UASDF. Different letters indicate significant differences (P < 0.05). *GAC* glucose adsorption capacity, *CAC* cholesterol adsorption capacity, *ASDF* soluble dietary fiber from pomelo peel by alkaline method, *UASDF* soluble dietary fiber from pomelo peel by ultrasound-assisted alkaline method.

#### Conclusion

In this study, alkali-extracted pomelo peel SDF was modified using ultrasound to improve its extraction and functional properties. Ultrasonic modification improved the hydration characteristics (WHC, OHC and SC) of ASDF. Structural characterization showed that ultrasonic modification altered the infrared characteristics of ASDF, decreased its crystallinity, and generated a porous structure. Compared to ADSF, UASDF had higher adsorption characteristics (GAC and CAC). These improved functional properties were attributed to the pore structure of the UASDF surface. In addition, ultrasonic modification improved the scavenging capacity of ABTS and ·OH radicals of ASDF, indicating enhanced antioxidant properties. According to the current study, grapefruit peel is a good source of SDF. SDF extraction by ultrasound-assisted alkali extraction has the potential to be used as an additive in the food industry for healthy living.

### Materials and methods Materials

Fresh white pomelos were purchased from Yibin Daily Shopping Supermarket (Sichuan, China), whose peels were stripped and washed, and cut into 2 cm pieces. Before extraction, the pomelo peels were dried in an oven at 60 °C until constant weight and ground to a fine powder using a pulverizer (HN-C1000, Ivana Good Electric Co., Ltd., China), passing through a 60 mesh sieve. Before extraction, the fat in pomelo peel powder was removed by soaking with 4 times the volume of petroleum ether, and then washing with 80% ethanol to remove the residual ether, after which the sample was dried in an oven at 50 °C (101-3HB, Beijing Zhongxing Weiye Instrument Co., Ltd., Beijing, China). Sodium hydroxide and anhydrous ethanol were obtained from Xilong Science Co., Ltd. (Shenzhen, Guangdong, China) and Shanghai Titan Technology Co., Ltd (Shanghai, China), respectively. All other reagents were of analytical grade.

#### Alkali treatment

The defatted pomelo peel powder was extracted with 3% (w/v) NaOH solution at a feed/liquid ratio of 1:30 g/ mL at 75 °C for 60 min. The supernatant was obtained by centrifugation at 1693  $\times$  g for 15 min, and it was precipitated using 95% ethanol (4:1, v/v) (Standing time was 8 h at 4 °C), and freeze-dried for 12 h. The SDF obtained from alkali treatment was ASDF.

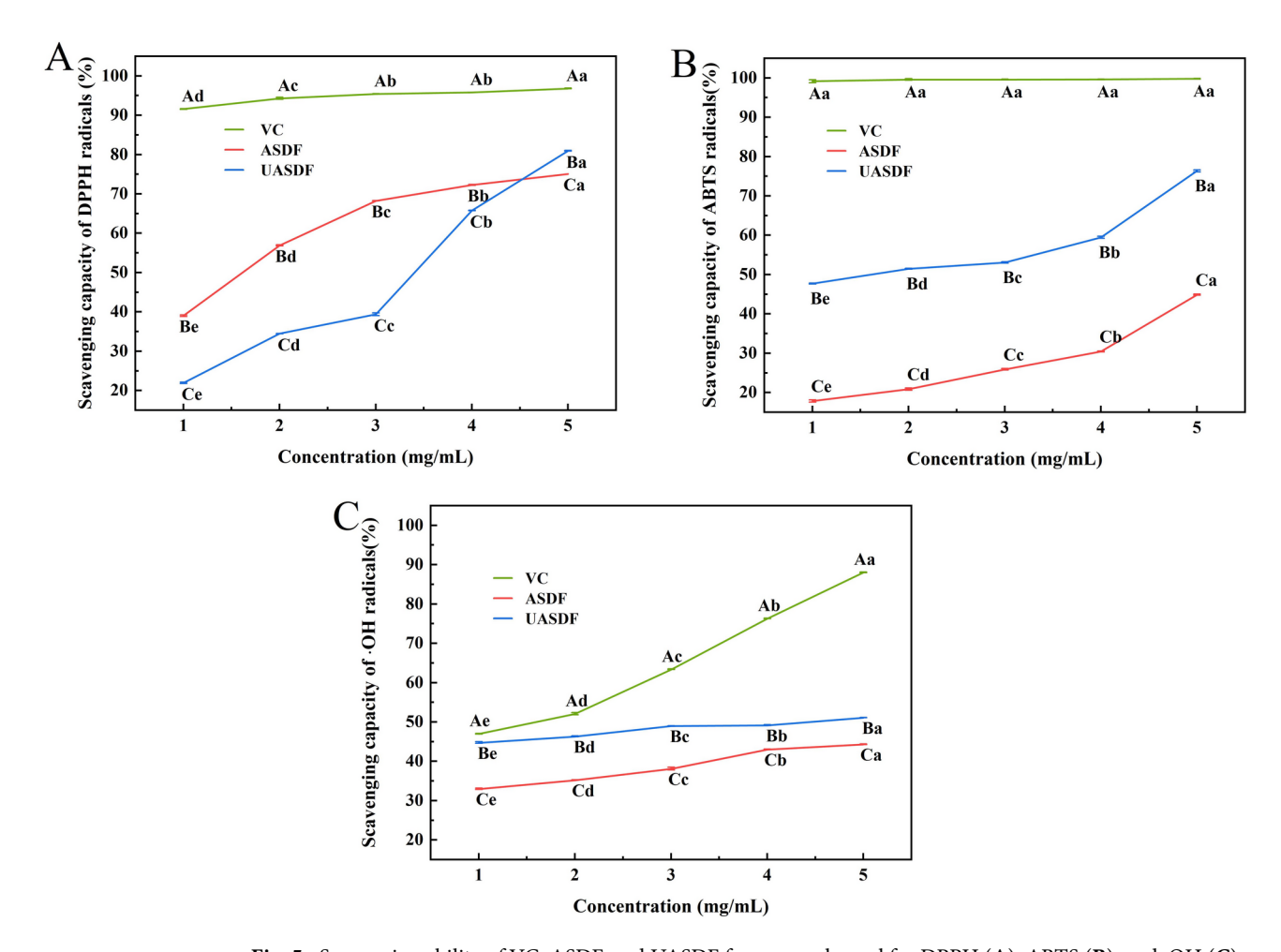


Fig. 5. Scavenging ability of VC, ASDF, and UASDF from pomelo peel for DPPH (A), ABTS (B), and ·OH (C). Different lowercase letters indicate within-group differences and different uppercase letters indicate between-group differences (P<0.05). ASDF soluble dietary fiber from pomelo peel by alkaline method. UASDF soluble dietary fiber from pomelo peel by ultrasound-assisted alkaline method.

#### Ultrasound modification

The pomelo peel powder was mixed with sodium hydroxide solution at feed/liquid of 1:30 g/mL according to the above conditions and ultrasonicated at 75 °C, 360 W for 60 min (KQ-700DE, Kunshan Ultrasonic Instrument Co., Ltd., Jiangsu, China). The supernatant was obtained by centrifugation at 1693  $\times$  g for 15 min, and it was precipitated using 95% ethanol (4:1, v/v) (Standing time was 8 h at 4 °C), and freeze-dried for 12 h. The ultrasound-assisted alkali treatment of dietary fiber was UASDF. ASDF and UASDF samples were stored in silica gel desiccators. The extraction rate formula for SDF samples was calculated as follows Eq. (1):

Yield (%) = 
$$\frac{m_1}{m_0} \times 100\%$$
 (1)

Where  $m_0$  is the mass of the dried sample (g),  $m_1$  is the mass of the dried SDF (g).

#### Physicochemical properties of SDF

Water holding capacity (WHC)

The WHC of ASDF and UASDF were determined according to the method described by Chen et al.<sup>39</sup>. Mixed 0.5 g SDF sample ( $W_1$ ) with 20 mL of distilled water and absorbed for 1 h at room temperature. Subsequently, the sample was centrifuged at 2441 × g for 10 min, and the precipitate was collected and weighed ( $W_2$ ). The WHC was calculated as follows Eq. (2):

WHC (g/100g) = 
$$\frac{W_2 - W_1}{W_1} \times 100\%$$
 (2)

Oil holding capacity (OHC)

The OHC of the samples was determined according to the description of Chen et al.<sup>39</sup>. The SDF sample (0.5 g,  $M_1$ ) was added to 10 mL of soybean oil and reacted for 1 h at room temperature. Subsequently, the mixture was

centrifuged at 1867  $\times$  g for 15 min. Ultimately, the supernatant was discarded and measured (M<sub>2</sub>). The OHC was calculated as follows Eq. (3):

OHC (g/100g) = 
$$\frac{M_2 - M_1}{M_1} \times 100\%$$
 (3)

Swelling capacity

0.2 g SDF sample ( $W_1$ ) was hydrated with 10mL water in a graduated test tube and the volume ( $V_1$ ) was recorded. After 18 h of hydration, the volume ( $V_2$ ) was recorded and calculated by the following equation 40. The SC was calculated as follows Eq. (4):

$$SC (mL/g) = \frac{V_2 - V_1}{W_1}$$
 (4)

#### Structural characteristics

Fourier transform infrared (FT-IR) spectroscopy

FT-IR spectra of dietary fibers were determined using a Nicolet 6700 spectrometer (Bruker, Germany). The samples were mixed with KBr, ground into powder, and pressed into round tablets. Each spectrum had a resolution of  $4 \, \mathrm{cm}^{-1}$  and was scanned 64 times with wave numbers ranging from 500 to 4000 cm<sup>-141</sup>.

X-ray diffraction

X-ray diffraction was referenced and slightly modified from  $^{42}$ . The crystalline structure of ASDF and UASDF samples was determined using X-ray diffraction (EMPYREAN, PANalytical B.V., Netherlands) operated at 30kv and 10 mA. The diffraction angle (2 $\theta$ ) was scanned from 10° to 60° in 0.02 increments at a rate of 5°/min. The crystallinity of the sample was calculated using diffraction intensity data using the method of Segal et al.  $^{43}$ . The CrI was calculated as follows Eq. (5):

$$CrI = \frac{I_{002} - I_{am}}{I_{002}} \times 100\%$$
 (5)

Where CrI is the relative crystallinity (%),  $I_{002}$  is the maximum intensity (in arbitrary units) of the 002 lattices at  $2\theta$  °and  $I_{am}$  is the lowest intensity of diffraction in the same units at  $2\theta$ =18°-19°.

Scanning electron microscopy (SEM)

The surface and microstructure of ASDF and UASDF were determined by SEM (JSM-7500 F, JEOL, Japan) at 15 kv. The dehydrated samples were placed on double-sided conductive tape covered with a 10 nm gold layer, and representative photographs of the samples were taken at 200x and 1000x magnification.

#### **Functional characteristics**

Glucose adsorption capacity (GAC)

The glucose adsorption capacity of the samples was determined as described by Qiao et al.  $^{44}$ . The sample (0.5 g) was dissolved in 20 mL of glucose solution (100 mmol/L) and mixed in a shaker at 37 °C, 120 rpm for 2 h (QYC-2102 C, Shanghai Fuma Experimental Equipment Co., Ltd., Shanghai, China), and then centrifuged at 2441 × g for 20 min. Take 1 mL of supernatant and 2 mL DNS color development solution mixed well and immersed in 100 °C for 6 min. After cooling in ice water, 9 mL of distilled water was added for dilution, and the absorbance was measured at 540 nm after mixing well (UV-1900i, Shimadzu, Japan), and quantified according to the glucose standard curve (Y = 1.379X + 0.016 and  $R^2$  = 0.999). The GAC was calculated as follows Eq. (6):

$$GAC (mg/g) = \frac{m_1 - m_2}{M}$$
 (6)

Where  $m_1$  is unadsorbed glucose mass (mg),  $m_2$  is adsorbed glucose mass in the supernatant (mg), and M is the mass of SDF (g).

Cholesterol adsorption capacity (CAC)

The yolk from a fresh egg was mixed into an emulsion with water at 1:9 (v/v). 0.5 g SDF sample was added twice to 20 mL of egg yolk solution, adjusted to pH = 2 and pH = 7, and shaken for 2 h in a 120 rpm shaker environment at a temperature of 37  $^{\circ}$ C. The supernatant was taken and centrifuged at 1693 × g for 20 min, and the absorbance was measured at 550 nm according to the o-phthalaldehyde method. Cholesterol adsorption capacity of the samples was measured as described by Zhang et al.<sup>45</sup>. 100  $\mu$ L of the sample was taken and 900  $\mu$ L of 90% glacial acetic acid, 0.2 ml of o-phthalaldehyde, and 4mL of concentrated sulphuric acid were added sequentially. The mixture was homogenised and allowed to stand for 10 min, and the absorbance was measured at 550 nm. The cholesterol content was calculated according to the cholesterol standard curve (Y = 0.021X + 0.045 and R²=0.999). The CAC was calculated as follows Eq. (7):

$$CAC (mg/g) = \frac{m_1 - m_2}{M}$$
 (7)

Where  $m_1$  is the cholesterol content in the egg yolk solution before adsorption (mg),  $m_2$  is the cholesterol content in the egg solution after adsorption (mg), and M is the mass of SDF (g).

Determination of antioxidant capacity

DPPH, ABTS, and hydroxyl radical assay were determined according to the method of Zhao et al. 46, Chen et al. 47, and Hernández-Corroto et al. 48 with slight modifications.

<u>DPPH radical scavenging assay</u> Anhydrous methanol was used to configure 0.1 mmol/L DPPH solution. 2 mL sample solution at various concentrations (1, 2, 3, 4, and 5 mg/mL) was mixed with 2 mL of DPPH solution. The mixture was reacted under dark conditions for 30 min. and then the absorbance was measured at 517 nm. VC was used as a positive control. The DPPH radical scavenging rate was calculated according to the following equation Eq. (8):

Scavenging activity (%) = 
$$\left(1 - \frac{A_1 - A_2}{A_0}\right) \times 100$$
 (8)

Where  $A_0$  is the absorbance of distilled water.  $A_1$  is the absorbance of the sample solution group.  $A_2$  is the absorbance of the sample without DPPH solution .

ABTS radical scavenging assay 0.4 mL sample solution at various concentrations (1, 2, 3, 4, and 5 mg/mL) were mixed with 3.6 mL of ABTS working solution. The reaction was kept in a dark place for 30 min, and the absorbance value was measured as  $A_1$  at 734 nm. VC was used as a positive control. The ABTS radical scavenging rate was calculated according to the following equation Eq. (9):

Scavenging activity (%) = 
$$\left(1 - \frac{A_1 - A_2}{A_0}\right) \times 100$$
 (9)

Where  $A_0$  is the absorbance of distilled water and buffer.  $A_1$  is the absorbance of the sample solution group.  $A_2$  is the absorbance of the sample without ABTS solution.

Hydroxyl radical scavenging capacity 1 mL SDF sample solution at various concentrations (1, 2, 3, 4, 5 mg/ mL), was mixed with 1 mL of 6 mmol/L ferrous sulfate, 1 mL of 6 mmol/L salicylic acid solution, and 1 mL of 3% v/v  $\text{H}_2\text{O}_2$  solution. Then the reaction was carried out at 37 °C for 20 min, and the absorbance was measured at 510 nm after cooling. VC was used as a positive control. The hydroxyl radical scavenging rate was calculated according to the following equation Eq. (10):

Scavenging activity (%) = 
$$\left(1 - \frac{A_1 - A_2}{A_0}\right) \times 100$$
 (10)

Where  $A_0$  is the absorbance of distilled water.  $A_1$  is the absorbance of the sample solution group.  $A_2$  is the absorbance of distilled water instead of  $H_2O_2$  solution.

#### Statistical analysis

Statistical analyses were performed using SPSS 26.0 (SPSS Inc., Chicago, IL, USA) software. One-way analysis of variance (ANOVA) followed by a Duncan's multiple range tests was performed (P<0.05). All graphs in this study were obtained using Origin 2018. All experiments were repeated 3 times and results were expressed as means  $\pm$  standard error.

#### Data availability

The datasets used and/or analysed during the current study available from the corresponding author on reasonable request.

Received: 10 October 2024; Accepted: 25 April 2025

Published online: 01 June 2025

#### References

- Tocmo, R. et al. Valorization of pomelo (Citrus grandis Osbeck) Peel: A review of current utilization, phytochemistry, bioactivities, and mechanisms of action. Comp. Rev. Food Sci. Food Safe. 19, 1969–2012 (2020).
- Zhu, L. et al. An environmentally friendly carbon aerogels derived from waste pomelo peels for the removal of organic pollutants/ oils. Microporous Mesoporous Mater. 241, 285–292 (2017).
- 3. Howlett, J. F. et al. The definition of dietary fiber discussions at the Ninth Vahouny Fiber Symposium: building scientific agreement. Food Nutr. Res. 54, 5750 (2010).
- Martinez-Solano, K. C. et al. Ultrasound application for the extraction and modification of Fiber-Rich By-Products. *Food Eng. Rev.* 13, 524–543 (2021).
   Yuan, Z. et al. Effects of steam explosion on physicochemical, functional and structural properties of soluble dietary fiber from
- pomelo Peel. *Int. J. Food Eng.* **19**, 457–465 (2023).

  6. Chen, L. et al. Dietary fiber extraction from citrus Peel pomace: yield optimization and evaluation of its functionality, rheological
- behavior, and microstructure properties. *J. Food Sci.* **88**, 3507–3523 (2023).

  7. Wang, K. et al. Effects of extraction methods on the structural characteristics and functional properties of dietary fiber extracted
- from Kiwifruit (*Actinidia deliciosa*). Food Hydrocoll. **110**, 106162 (2021).

  8. Yang, C. et al. Mixed fermentation of navel orange Peel by Trichoderma viride and Aspergillus Niger: effects on the structural and
- functional properties of soluble dietary fiber. *Food Bioscience*. **57**, 103545 (2024).

  9. Sun, J. et al. Ultrasound-assisted alkali extraction of insoluble dietary fiber from soybean residues. *IOP Conf. Ser. : Mater. Sci. Eng.* **392**, 052005 (2018)

- 10. Kumar, K., Srivastav, S. & Sharanagat, V. S. Ultrasound assisted extraction (UAE) of bioactive compounds from fruit and vegetable processing by-products: A review. *Ultrason. Sonochem.* **70**, 105325 (2021).
- Li, S. et al. Influence of modification methods on physicochemical and structural properties of soluble dietary fiber from corn Bran. Food Chemistry: X. 14, 100298 (2022).
- 12. Geng, N. et al. Ultrasound-assisted enzymatic extraction of soluble dietary fiber from fresh corn bract and its physio-chemical and structural properties. *Qual. Assur. Saf. Crops Foods.* 14, 119–130 (2022).
- Dhar, P. & Deka, S. C. Effect of ultrasound-assisted extraction of dietary fiber from the sweetest variety queen pineapple waste of Tripura (India). J. Food Process. Eng. 46, e14220 (2023).
- 14. Fan, X. et al. Effects of ultrasound-assisted enzyme hydrolysis on the microstructure and physicochemical properties of Okara fibers. *Ultrason. Sonochem.* **69**, 105247 (2020).
- 15. Gan, J. et al. Comparison of structural, functional and in vitro digestion properties of bread incorporated with grapefruit Peel soluble dietary fibers prepared by three microwave-assisted modifications. *Food Funct.* 11, 6458–6466 (2020).
- Ibrahim, M. S. et al. Optimization of ultrasound assisted extraction and characterization of functional properties of dietary fiber from oat cultivar S2000. LWT 197, 115875 (2024).
- 17. Mall, U. P. & Patel, V. H. Carrot pomace powder: a promising source of polyphenols and prebiotics for improving gut health. *Nutrire* 49, 9 (2024).
- 18. Hua, X. et al. Effects of high-speed homogenization and high-pressure homogenization on structure of tomato residue fibers. *Food Chem.* **232**, 443–449 (2017).
- 19. Elleuch, M. et al. Dietary fibre and fibre-rich by-products of food processing: characterisation, technological functionality and commercial applications: A review. Food Chem. 124, 411–421 (2011).
- 20. Kumari, T., Das, A. B. & Deka, S. C. Impact of extraction methods on functional properties and extraction kinetic of insoluble dietary fiber from green pea peels: A comparative analysis. *Food Process. Preserv.* 46, (2022).
- Chen, H. et al. Effects of extrusion on structural and physicochemical properties of soluble dietary fiber from nodes of lotus root. LWT 93, 204–211 (2018).
- 22. Lin, D. et al. Effects of microbial fermentation and microwave treatment on the composition, structural characteristics, and functional properties of modified Okara dietary fiber. *LWT* **123**, 109059 (2020).
- Dong, W. et al. Chemical composition, structural and functional properties of soluble dietary fiber obtained from coffee Peel using different extraction methods. Food Res. Int. 136, 109497 (2020).
- 24. Zhang, Y., Liao, J. & Qi, J. Functional and structural properties of dietary fiber from citrus Peel affected by the alkali combined with high-speed homogenization treatment. LWT 128, 109397 (2020).
- Zhang, W. et al. Properties of soluble dietary fiber-polysaccharide from Papaya Peel obtained through alkaline or ultrasoundassisted alkaline extraction. Carbohydr. Polym. 172, 102–112 (2017).
- Zhang, J. et al. Extraction of *Heracleum dissectum* soluble dietary fiber by different methods: structure and antioxidant properties. J. Food Sci. 89, 3400–3411 (2024).
- Wei, E. et al. Microwave-assisted extraction releases the antioxidant polysaccharides from Seabuckthorn (*Hippophae rhamnoides* L.) berries. *Int. J. Biol. Macromol.* 123, 280–290 (2019).
- 28. Gan, J. et al. Microwave assisted extraction with three modifications on structural and functional properties of soluble dietary fibers from grapefruit Peel. *Food Hydrocoll.* **101**, 105549 (2020).
- noers from graperruit reel. *Food Hydrocoli*. **101**, 105549 (2020).

  29. Ma, Q. et al. Effects of different treatments on composition, physicochemical and biological properties of soluble dietary fiber in buckwheat Bran. *Food Bioscience*. **53**, 102517 (2023).
- 30. Aguado, R. et al. The relevance of the pretreatment on the chemical modification of cellulosic fibers. *Cellulose* **26**, 5925–5936 (2019).
- Jia, M. et al. Structural characteristics and functional properties of soluble dietary fiber from defatted rice Bran obtained through Trichoderma viride fermentation. Food Hydrocoll. 94, 468–474 (2019).
- 32. Luo, X. et al. Hydration properties and binding capacities of dietary fibers from bamboo shoot shell and its hypolipidemic effects in mice. *Food Chem. Toxicol.* **109**, 1003–1009 (2017).
- 33. Peng, F. et al. Physicochemical property, and functional activity of dietary Fiber obtained from Pear fruit pomace (Pyrus ussuriensis Maxim) via different extraction methods. *Foods* 11, 2161 (2022).
- 34. Xu, H. et al. In vitro binding capacities and physicochemical properties of soluble fiber prepared by microfluidization pretreatment and cellulase hydrolysis of Peach pomace. LWT Food Sci. Technol. 63, 677–684 (2015).
- 35. Wang, Z. B. et al. Fractionation, physicochemical characteristics and biological activities of polysaccharides from Pueraria lobata roots. *J. Taiwan Inst. Chem. Eng.* **67**, 54–60 (2016).
- 36. Domínguez-Rodríguez, G., Marina, M. L. & Plaza, M. Enzyme-assisted extraction of bioactive non-extractable polyphenols from sweet Cherry (*Prunus avium L.*) pomace. Food Chem. 339, 128086 (2021).
- 37. Shang, Y. et al. Physical properties and functional characteristics of broccoli-soluble dietary fiber. Food Bioscience. 56, 103272 (2023).
- 38. Wei, C. et al. Effects of High-Temperature, High-Pressure, and ultrasonic treatment on the physicochemical properties and structure of soluble dietary fibers of millet Bran. Front. Nutr. 8, 820715 (2022).
- 39. Chen, Y. et al. Physicochemical properties and adsorption of cholesterol by Okra (Abelmoschus esculentus) powder. *Food Funct.* **6**, 3728–3736 (2015).
- 40. Sun, C. et al. Production and characterization of Okara dietary fiber produced by fermentation with *Monascus Anka. Food Chem.* 316, 126243 (2020).
- 41. Zheng, Y. et al. Effects of three biological combined with chemical methods on the microstructure, physicochemical properties and antioxidant activity of millet Bran dietary fibre. Food Chem. 411, 135503 (2023).
- 42. Yang, C. et al. Physicochemical structure and functional properties of soluble dietary fibers obtained by different modification methods from mesona chinensis Benth. Residue. Food Res. Int. 157, 111489 (2022).
- 43. Segal, L. et al. An empirical method for estimating the degree of crystallinity of native cellulose using the X-Ray diffractometer. *Text. Res. J.* 29, 786–794 (1959).
- 44. Qiao, H. et al. Modification of sweet potato (Ipomoea Batatas Lam.) residues soluble dietary fiber following twin-screw extrusion. Food Chem. 335, 127522 (2021).
- Zhang, N., Huang, C. & Ou, S. In vitro binding capacities of three dietary fibers and their mixture for four toxic elements, cholesterol, and bile acid. *J. Hazard. Mater.* 186, 236–239 (2011).
- Zhao, Z. et al. Physicochemical properties and biological activities of polysaccharides from the Peel of Dioscorea opposita thunb. Extracted by four different methods. Food Sci. Hum. Wellness. 12, 130–139 (2023).
- Chen, G. et al. Comparison of different extraction methods for polysaccharides from bamboo shoots (Chimonobambusa quadrangularis) processing by-products. *Int. J. Biol. Macromol.* 130, 903–914 (2019).
- 48. Hernández-Corroto, E., Marina, M. L. & García, M. C. Multiple protective effect of peptides released from Olea europaea and Prunus persica seeds against oxidative damage and cancer cell proliferation. *Food Res. Int.* **106**, 458–467 (2018).

#### Acknowledgements

This research was funded by the Science and Technology Bureau of Zigong City (2023YKY02).

#### **Author contributions**

Conceptualization, Z.L.; methodology, Y.Y.; software, F.C.; validation, Y.Y., J.X. and G.J.; formal analysis, F.C.; investigation, M.X.; resources, Y.W.; data curation, Y.L.; writing—original draft preparation, Y.Y.; writing—review and editing, F.C.; visualization, X.W.; supervision, Y.Y. All authors have read and agreed to the published version of the manuscript.

#### **Declarations**

#### Competing interests

The authors declare no competing interests.

#### Additional information

**Correspondence** and requests for materials should be addressed to Y.W. or X.W.

Reprints and permissions information is available at www.nature.com/reprints.

**Publisher's note** Springer Nature remains neutral with regard to jurisdictional claims in published maps and institutional affiliations.

Open Access This article is licensed under a Creative Commons Attribution-NonCommercial-NoDerivatives 4.0 International License, which permits any non-commercial use, sharing, distribution and reproduction in any medium or format, as long as you give appropriate credit to the original author(s) and the source, provide a link to the Creative Commons licence, and indicate if you modified the licensed material. You do not have permission under this licence to share adapted material derived from this article or parts of it. The images or other third party material in this article are included in the article's Creative Commons licence, unless indicated otherwise in a credit line to the material. If material is not included in the article's Creative Commons licence and your intended use is not permitted by statutory regulation or exceeds the permitted use, you will need to obtain permission directly from the copyright holder. To view a copy of this licence, visit <a href="http://creativecommons.org/licenses/by-nc-nd/4.0/">http://creativecommons.org/licenses/by-nc-nd/4.0/</a>.

© The Author(s) 2025